Bulletin of the Seismological Society of America, Vol. 107, No. 5, pp. 2151–2159, October 2017, doi: 10.1785/0120160213

Impact of Mesh and DEM Resolutions in SEM Simulation of 3D Seismic Response

by Saad Khan,* Mark van der Meijde, Harald van der Werff, and Muhammad Shafique

Abstract This study shows that the resolution of a digital elevation model (DEM) and model mesh strongly influences 3D simulations of seismic response. Topographic heterogeneity scatters seismic waves and causes variation in seismic response (amplification and deamplification of seismic amplitudes) at the Earth's surface. DEM resolution influences the accuracy and detail with which the Earth's surface can be represented and hence affects seismic simulation studies. Apart from the spatial resolution of a DEM, the mesh resolution, adopted in the creation of a 3D spectral element meshing, also changes the detailedness of surface topography. Working with high-resolution data is in most cases not possible on a regional scale because of its costliness in terms of time, money, and computation. In this study, we evaluate how low the resolution of DEM and mesh can become before the results are significantly affected. We simulated models with different combinations of DEM and mesh resolutions. The peak ground displacement (PGD) obtained from these simulations was compared with the PGD of the model with the finest mesh and DEM resolution. Our results show that any mesh or DEM resolution of 540 m or coarser will give unrealistic results. These results are valid for similar terrains as studied here and might not be directly applicable to regions with significantly different topography.

Introduction

The Earth's topography acts as a reflecting surface for seismic energy. Its variation in elevation leads to scattering and focusing of propagating waves (Lee *et al.*, 2008, Lee, Komatitsch, *et al.*, 2009). Previous studies (such as Hartzell *et al.*, 1994; Bouchon *et al.*, 1996; Spudich *et al.*, 1996; Assimaki *et al.*, 2005; Lee, Chan, *et al.*, 2009; Lee, Komatitsch, *et al.*, 2009; Hough *et al.*, 2010; Kumagai *et al.*, 2011; Takemura *et al.*, 2015) show that topography amplifies ground shaking at mountain ridges, whereas deamplification of ground motion has been observed in valleys. Recently, numerical simulations have been used to study the complicated phenomena of scattering and its effects on ground motion (e.g., Bouckovalas and Papadimitriou, 2005; Lee *et al.*, 2008; Lee, Komatitsch, *et al.*, 2009; Maufroy *et al.*, 2015; Takemura *et al.*, 2015).

There is a wide range of digital topography representation, commonly referred to as the digital elevation model (DEM). The (spatial) resolution is a property of the DEM (Smith *et al.*, 2006; Sørensen and Seibert, 2007; Wu *et al.*, 2008). DEMs come in various resolutions, ranging from fine (e.g., light detection and ranging [lidar] at ∼12 cm) to coarse (e.g., Global 30 Arc-Second Elevation [GTOPO30] at ∼1 km) (see Data and Resources). The DEM resolution sets a limitation on the realism of topographic data. For example, coarse resolution data smoothen topography and result in a loss of topographic features (Shafique *et al.*, 2008; Vaze *et al.*, 2010; Shafique, van der Meijde, Kerle, *et al.*, 2011). Shafique *et al.* (2008) evaluated the impact of DEM resolution and its derived attributes on topographic representation and derived seismic response. Their study shows that DEM source and spatial resolution have an effect on the computed output. However, the study was based on topography-derived proxies and lacked simulation.

A DEM resolution and the representation of that DEM on various mesh resolutions when used for 3D numerical modeling approaches become more important in regional studies (e.g., hundreds of km^2). Existing models such as U.S. Geological Survey (USGS) ShakeMap and Prompt Assessment of Global Earthquakes for Response (PAGER) are at a coarse resolution of 1 km (Jaiswal *et al.*, 2009), thus giving generalization (Vaze *et al.*, 2010). On the other hand, geotechnical studies evaluating the impact of topography with higher resolution are limited to a small spatial scale. A coarse resolution may save time but come at a cost of accuracy, whereas a fine resolution may ensure accuracy but come at a cost of applicability (i.e., cannot be applied to a regional scale investigation).

For performing 3D numerical simulations such as the spectral element method (SEM), a 3D geometrical model

*Also at Department of Geology, Bacha Khan University Charsadda, P.O. Box 20, Charsadda, Khyber Pakhtunkhwa, Pakistan.

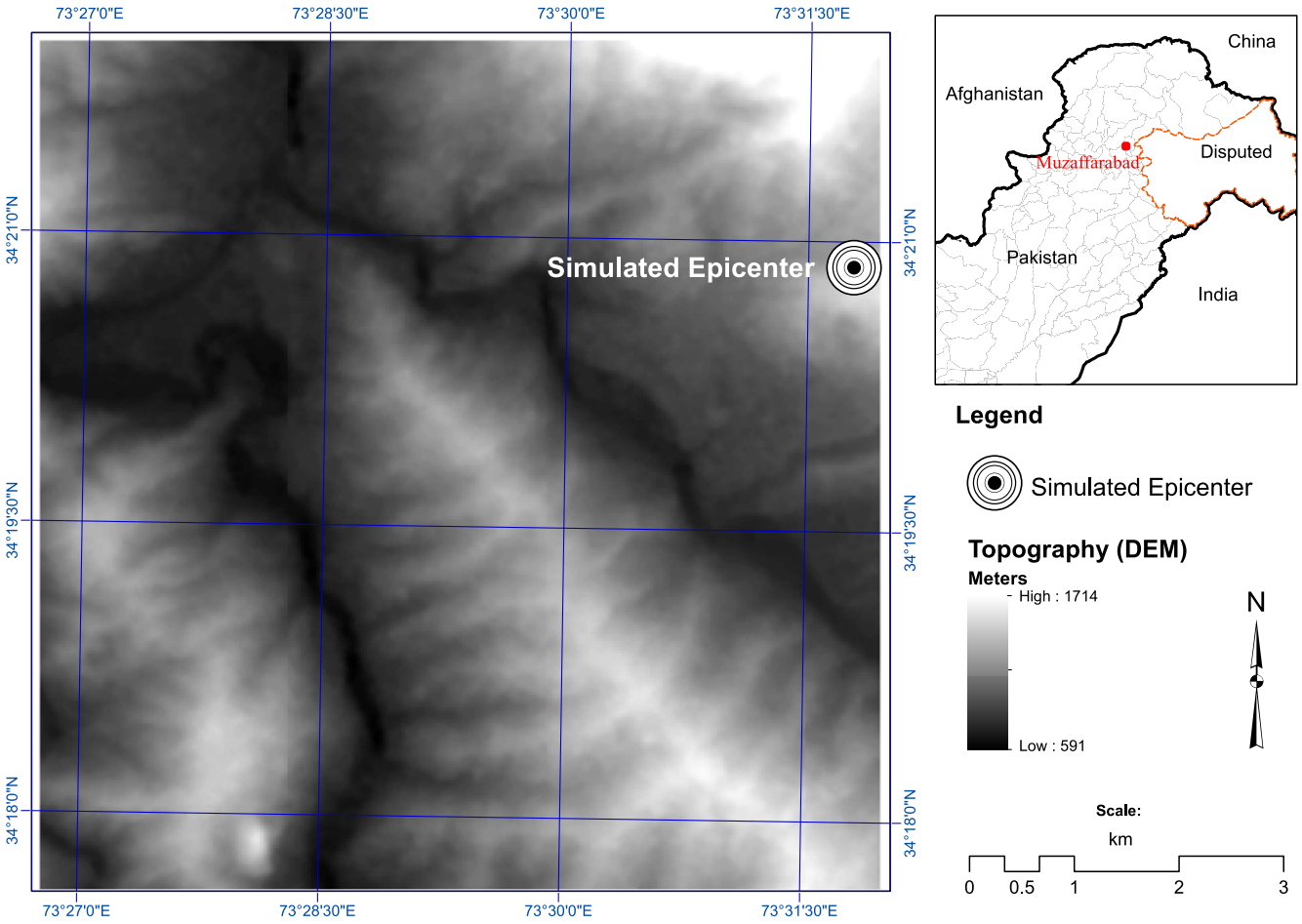

Figure 1. Digital elevation model (DEM) of the study area, including the simulated earthquake epicenter, shifted to fit in the model. The color version of this figure is available only in the electronic edition.

is prepared from a DEM that represents the topographic surface. The 3D model is then meshed with a hexagonal mesh (which consists of hexahedra elements). The mesh is defined by material and structural properties that define how it will react to applied conditions (e.g., an earthquake). The meshed model is then taken to a simulator (SPECFEM3D in this study), which produces simulated output. The hexagonal mesh is required to have a suitable resolution that could correctly resolve the surface obtained from a DEM in a 3D geometric model. For example, a model created with a 30 m DEM when meshed with a coarser resolution would not be able to correctly resolve the surface, and hence many small-scale topographic features would be left out. It is thus necessary to take into account both DEM and mesh resolution when performing such studies.

Theoretically, a model with the finest mesh and DEM resolution should provide the best possible result. At the same time, fine resolution models require a large amount of computational power and hence may not always be possible. High-resolution DEM availability and related costs may also be an issue. Thus, it is important to know how coarse a mesh and/or DEM resolution can be while still providing realistic results (compared as though it were calculated with the highest possible resolutions). Efficient use of time and computation must be considered, and therefore the generated result should still be applicable regionally. Therefore, the goal of this study is to find the coarsest mesh and/or DEM resolution that can be used in a 3D numerical simulation involving regional scale topography, without compromising accuracy.

Area, Data, and Method

Area

We selected a study area around the city of Muzaffarabad in northern Pakistan (Fig. 1). The area consists of rugged terrain with high relief and showed manifestations of topographic amplification during the 2005 Kashmir earthquake (Shafique *et al.*, 2008). We focused on a single ridge trending northwest–southeast. Its ridge crest is perpendicular to the direction of wave propagation. The setting allows us to study the effects of valleys and ridges in an isolated and controlled environment.

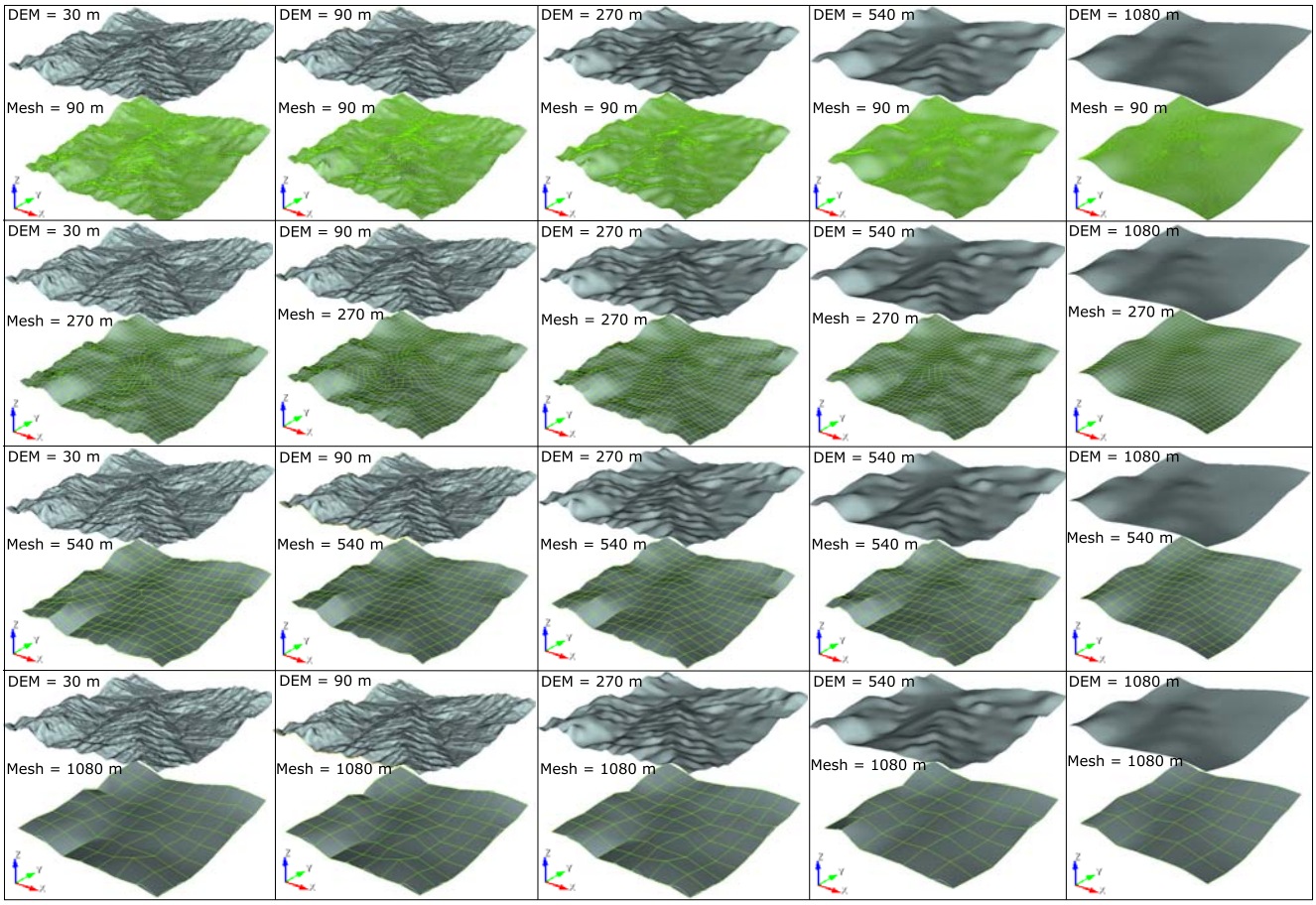

Figure 2. Study area in bird's-eye view (looking northwest) showing a graphical representation of different combinations of DEM and mesh resolutions on which spectral element method (SEM) test was performed. Top surface is the DEM-derived topographic surface, whereas the same surface after meshing is shown below it. The DEM-derived surface gets smoothed by losing fine features when the DEM gets coarsened (left to right). The DEM-derived topographic surface at 30 m resolution contains fine topographic features which disappear when the surface is smoothed as a result of DEM coarsening. The DEM-derived topographic surface gets accurately resolved with the fine meshes. The color version of this figure is available only in the electronic edition.

Data

We acquired an Advanced Spaceborne Thermal Emission and Reflection Radiometer global digital elevation model of 30 m spatial resolution (see Data and Resources). The original 30 m resolution was resampled with a pixel aggregate technique to 90, 270, 540, and 1080 m. In this technique, the individual values within a group of pixels were aggregated by calculating the mean to produce a single coarser resolution pixel of the mean value. Each of these DEM resolutions were then resolved with mesh resolutions of 90, 270, 540, and 1080 m, constituting a total of 20 models (Fig. 2). Models meshed with 90 m can resolve maximum frequencies up to ~16.6 Hz, 270 m up to ~5.5 Hz, 540 m up to ~2.7 Hz, and 1080 m up to ~1.4 Hz. The number of Gauss–Lobatto–Legendre points per grid spacing was kept at 5.

To create a 3D geometrical model for each of the tests, we used software package Cubit v.13.0 (see Data and Resources). Cubit is a software toolkit for the generation of 2D and 3D finite-element meshes.

In this study, we incorporated a DEM to the mesh and extended the mesh to a depth of 7 km. The topographic surface was set as a free surface; the rest of the five plane surfaces were set as absorbing surfaces. The models were meshed with a hex meshing technique with refining (when required) near the topographic surface to make sure there are no deformed elements.

Method

For mesh generation, Cubit is used in conjunction with GeoCubit. GeoCubit is python-based software developed at Istituto Nazionale di Geofisica e Vulcanologia (INGV), which automates the mesh generation process. The automated process involves three major steps. The first step is the construction of a 3D geometry. GeoCubit creates points from a DEM, combines these points to make lines, and eventually creates a surface by combining the lines. After creating the topographic surface, a 3D geometrical model is created. The second step is meshing the geometry. After creation of the 3D geometrical model, the model is meshed with hexa-

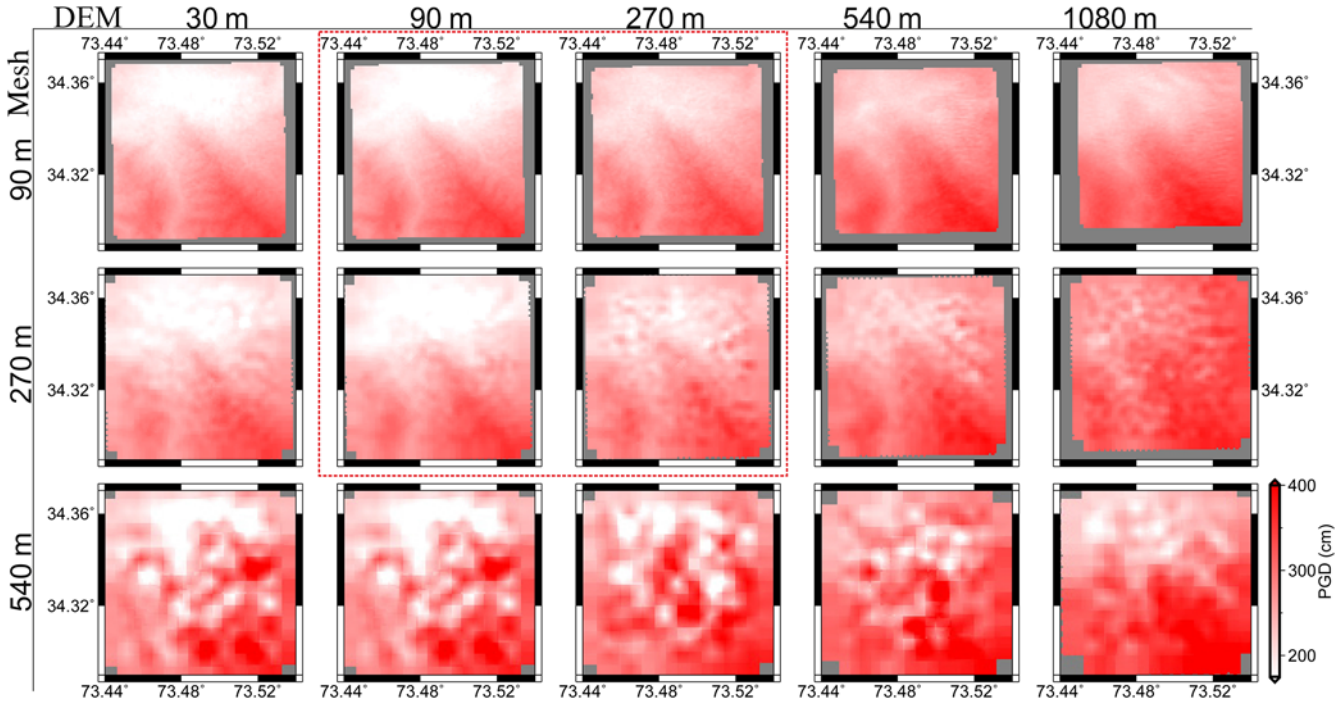

Figure 3. Peak ground displacement (PGD) of 15 tests out of a total 20 carried out in this study. Images in rows 1, 2, and 3 belong to models meshed with 90, 270, and 540 m, respectively. Images in columns 1, 2, 3, 4, and 5 belong to models using DEM of 30, 90, 270, 540, and 1080 m, respectively. The color version of this figure is available only in the electronic edition.

hedral elements. The last step involves defining boundary conditions and mesh export for simulation.

Mesh elements were exported to a format readable by the simulator. All tests were simulated with SPECFEM3D Cartesian, which is capable of simulating acoustic, elastic, coupled acoustic/elastic, poroelastic, or seismic-wave propagation in any type of conforming mesh of hexahedra (see Data and Resources). We considered a point-source data represented by the centroid moment tensor (CMT) solution of the 2005 Kashmir earthquake acquired from the Global CMT catalog (see Data and Resources). Because we performed an analysis to evaluate the impact of the resolution of models rather than simulating the actual effect of the earthquake, we moved the source to a position where it was optimally located to study the effect of DEM and model resolution on topographic amplification. The original location was changed to bring the source inside the model, and in a direction perpendicular to the targeted ridge's crest (Fig. 1). A delta source time function was used by keeping the half duration at 0. The changing mesh resolution changes source frequencies from 5.5 Hz for the 90 and 270 m mesh to 2.7 Hz for the 540 m mesh and finally to 1.4 Hz for the 1080 m mesh. The moment tensor parameters were kept constant in each simulation. Because of unavailability of a realistic wavespeed model for the area, we assigned constant wavespeeds ($V_P = 2800$ m/s, $V_S = 1500$ m/s) and density ($\rho = 2300$ km/m^3), representative of upper crustal conditions, throughout the model and across all tests. Hence, for all tests, all parameters were kept constant, except the mesh and topography resolution (in order to isolate resolution effects on topographic amplification).

We analyzed peak ground displacement (PGD) to evaluate the effect of changing mesh and DEM resolution. PGD mostly relates to the relatively lower frequency component of earthquakes (Kramer, 1996) and at the same time, the SEM technique efficiently simulates low-frequency earthquake ground motion (Dhanya *et al.*, 2017). It was assumed that a fine DEM represents topography with higher accuracy, and when resolved with a fine mesh would give our reference realistic output.

Results and Discussion

The DEM data are incorporated to Cubit as point data. These points are then joined with a smooth line and eventually a surface is created based on these lines. In this process, the DEM-derived surface gets smoothed by losing fine features when the DEM gets coarsened as shown in Figure 2. The combination of the highest resolution DEM and mesh contains small-scale topographic features, and the model is a close representation of the true topography at 30 m resolution. These fine features disappear and the surface is smoothed when the DEM resolution coarsens (going from left to right in Fig. 2). When keeping the DEM resolution equal but varying the mesh resolution, we observe that the model is not capable of representing true topography properly anymore; the similarity is lost (going from top to bottom in Fig. 2). Features smaller than the mesh resolution are lost and consequently produce stair-stepwise features. These

features influence the simulation and produce artifacts. An example of such artifacts can be observed in Figure 3 at 540 m mesh resolution where the output does not match the topography. Chances of stair-stepwise features are increased when a fine resolution DEM-derived surface is resolved with a coarser mesh. Vice versa, when a coarser DEM-derived topographic surface is resolved with a finer mesh, the surface is accurately resolved and the simulation produces output without any artifacts.

For analyzing the impact of mesh and DEM resolution, we show PGD (Fig. 3) obtained from 15 (out of 20) combinations of mesh and DEM resolutions shown in Figure 2. Results from the 30 m mesh are unavailable due to computational limitations. We refer to each model output with a code. A resulting model based on a mesh of 90 m and a DEM of 30 m would be mentioned as m90d30. Because this model is the result of the finest mesh and DEM resolution, it has therefore been taken as a reference for other models in comparison and analysis.

Upon visual analysis of the PGD images (Fig. 3), we can see that the effect of ridges and valleys gets smoother when the DEM gets coarsened (left to right). High amplitudes of PGD can be seen in the southeast of the images, which corresponds with the topography of the area (Fig. 1). This amplitude's pattern is consistent with previous studies on topographic amplification that show high amplitudes at ridges and lower amplitudes in valleys (e.g., Hartzell *et al.*, 1994; Bouchon *et al.*, 1996; Spudich *et al.*, 1996; Assimaki *et al.*, 2005; Lee, Komatitsch, *et al.*, 2009; Hough *et al.*, 2010; Kumagai *et al.*, 2011; Takemura *et al.*, 2015). This effect is more pronounced in images obtained from models meshed with 90 and 270 m (row1 and row2, respectively). With the increase of mesh resolution to 540 m, and further, the correlation between amplitudes and topography becomes less pronounced.

We observe a general trend of increasing amplitudes with coarsening DEM resolution. This trend is because of the scattering effect of detailed irregularities at the topographic surface. At finer resolutions, there is an abundance of irregularities at the surface. These small irregularities on slopes interfere with incoming seismic waves in a destructive manner, lead to additional scattering of the upward-moving seismic waves, and prevent it from focusing, thus resulting in lower amplitudes. When the DEM/mesh resolution is relatively coarse, any irregularities smaller than its resolution are smoothed (Shafique, van der Meijde, Kerle, *et al.*, 2011) and destructive interferences are reduced, resulting in higher amplitudes. Coarsening of the mesh resolution to 540 m and beyond results in an inaccurate representation of topography, and, in turn, gives inaccurate information about ground response.

Results show more differences in terms of feature response if there is a change in DEM resolution compared with a change in mesh resolution at the same resolution ratio. It is because the hexahedral meshes have the ability to adjust their geometry to the input topographic data, even when meshed at coarser resolution. Therefore, even if the mesh resolution is coarser than the resolution of the DEM, it is still possible to maintain a realistic representation of the actual topography.

We compare the output of each of the 14 models (referrals) with the output of model m90d30 (the reference) (Fig. 4). The scatter plots show PGD amplitudes between the reference and referral image. The PGD of the reference (m90d30) is on the x axes, whereas the referral images are on the y axes. Slope, intercept, R^2, ordinary least square (OLS), and best-fit lines for each referral are given with the respective plots. Increased scattering (with respect to best-fit line) has been observed when the DEM resolution is changed, compared with change in mesh resolution at the same ratio. Based on the spatial images and statistical data, we set criteria for an acceptable range of DEM and mesh resolutions. A first criterion for acceptance is that the output must follow the topographic features in the response (i.e., high amplitudes on ridge crest and low amplitudes in valleys). Using this criterion, it was found that any model meshed with a resolution of 540 m or coarser is unacceptable (Fig. 3). The second and third criteria of acceptability are based on statistics. The perfect-fit 1-to-1 line is an indicator of a perfect match between the reference and referral image (i.e., both have the same data). Slope, intercept, and R^2 of the best-fit line indicate how the referral image is different from the reference image. They show that with coarsening of mesh or DEM resolution, the accuracy decreases. This decrease can be interpreted from the decrease in R^2, change in slope from 1, and shift of best-fit line from the perfect-fit line. OLS also indicates that, while coarsening the DEM and/or mesh resolution, the error in amplitude increases. The last criterion is that the best-fit line must touch the perfect-fit line. Overall, we set that the slope must be 1.0 ± 0.15, R^2 must be greater than 0.90, and OLS cannot be greater than 20. Models not fulfilling these criteria are considered to be inaccurate/unrealistic and therefore unacceptable. Based on these criteria of acceptability, any model based on a 540 m or coarser mesh and/or DEM generate unacceptable/unrealistic results. The criteria of acceptance can also be expressed in terms of the ratio of each combination of mesh and DEM resolution with respect to the finest resolution (Fig. 5). We do our selection based on the criteria that the majority of an area must have a ratio of less than 0.2 (20%), with respect to 1.0. It can be noted that models with DEM resolutions of 30, 90, and 270 m at mesh resolution of 90 and 270 m have the majority of their area at ratio values of less than 0.2. A further increasing of the DEM resolution results in an increase in spatial extent of higher ratios. At the same time, a further increase in mesh resolution results in extreme ($\gg 0.2$) ratio values.

The following discussion focuses on changes that occurred due to mesh and DEM changes within the acceptable resolution range, but as coarse as possible. We selected four model outputs, each with a combination of 90 and 270 m DEM and mesh resolutions (marked in Fig. 3), to understand how changes occur between models with varying mesh and DEM resolution (Figs. 6 and 7).

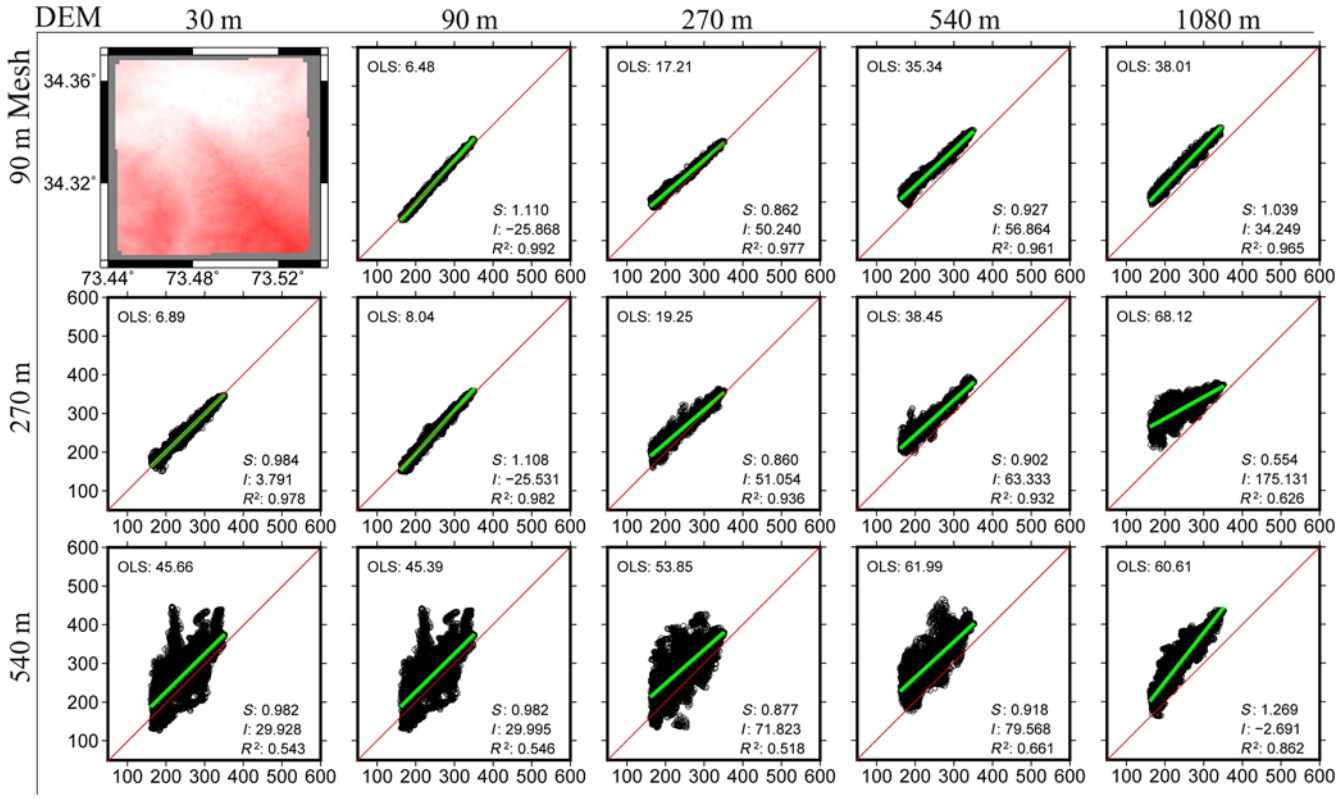

Figure 4. Scatter plots of PGD of reference model (x axis) against PGD of 14 tests (y axis). (top left) m90d30 is the reference model. Statistical data for each model are also given in the bottom right corner of each image. OLS, ordinary least square. The color version of this figure is available only in the electronic edition.

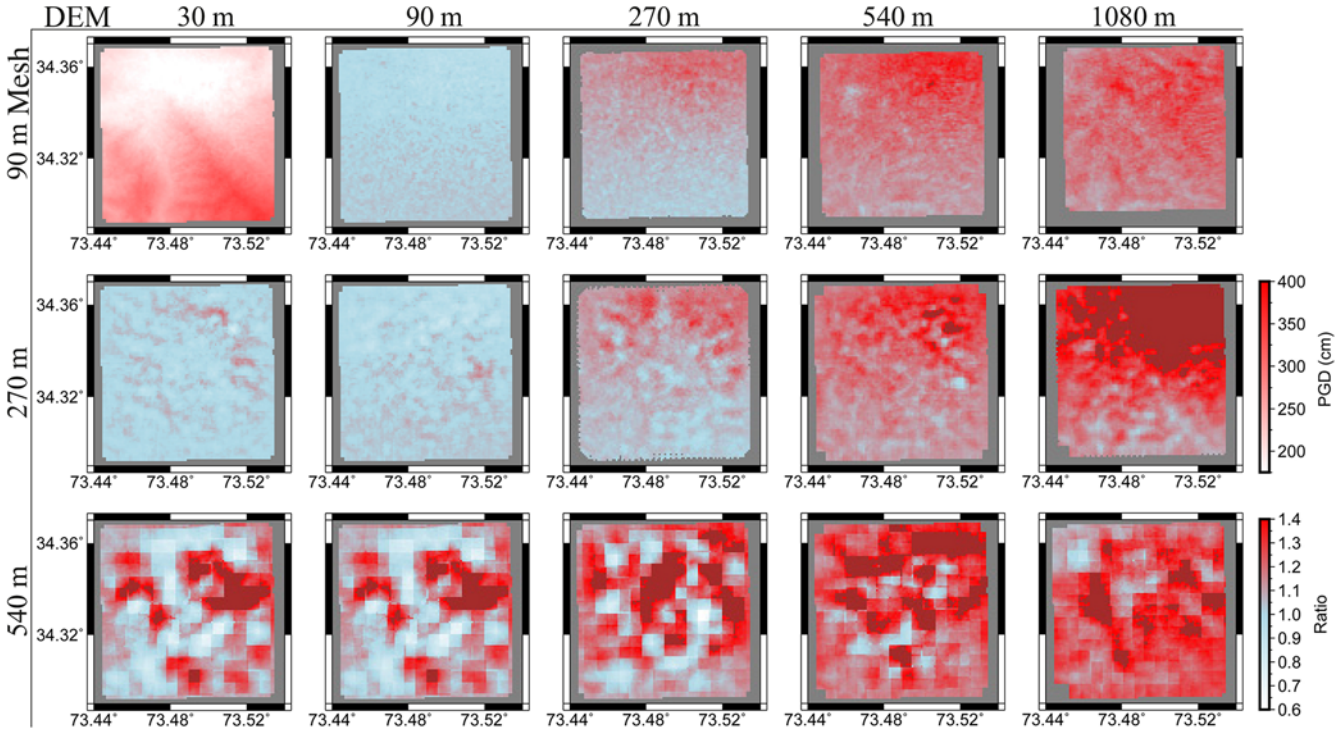

Figure 5. Ratios of each model with reference model (m90d30) of the finest mesh and DEM combination. The color version of this figure is available only in the electronic edition.

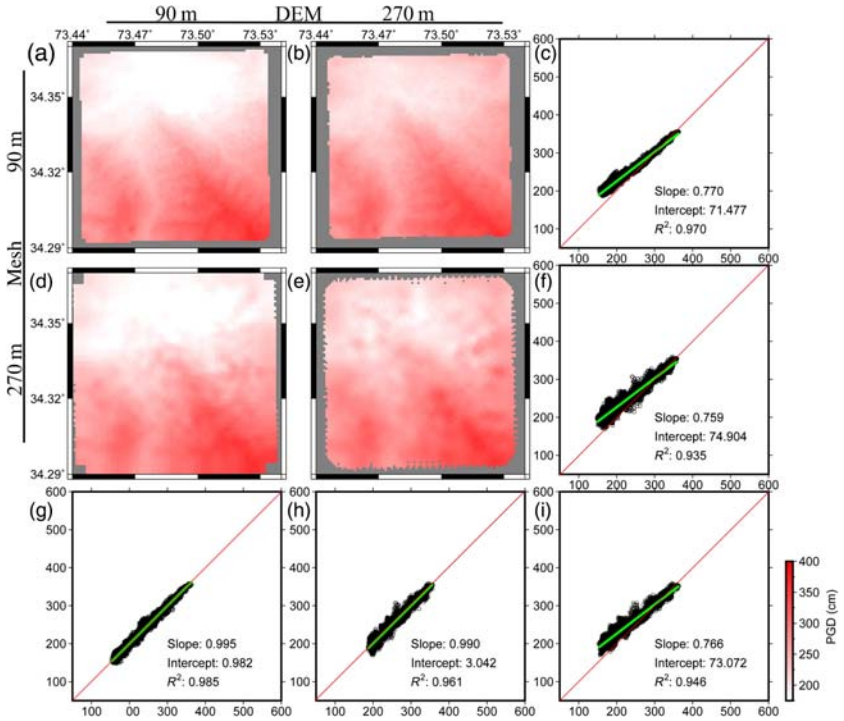

Figure 6. Scatter plots between models of 90 and 270 m mesh and DEM resolutions. (g) Scatter plot is product of (a) m90d90 and (d) m270d90, (h) plot of (b) m90d270 and (e) m270d270, (i) plot of (a) m90d90 and (e) m270d270, (f) plot of (d) m270d90 and (e) m270d270, (c) plot of (a) m90d90 and (b) m90d270. The color version of this figure is available only in the electronic edition.

In the scatter plots in Figure 6, we observe that m90d90 and m270d90 give the most similar results of all comparisons. The statistics based on the scatter plot give a best-fit and R^2 of almost 1.0, and the intercept is very close to 0. An almost comparable good correlation is found between m90d270 and m270d270. This clearly indicates that changing the mesh from 90 to 270 m has very little impact on the modeled results. For the other two comparisons, we see that R^2 is also close to 1.0, but for the slope and the intercept we observe larger variations. The slope decreases to around 0.75 and the intercepts are in the 70–75 range. We observe there an overestimation of the lower PGD values, compared with m90d90. So, changing mesh resolution has less impact than changing the DEM resolution for this range of resolutions.

In the ratio images (Fig. 7), we show ratios for the same images as Figure 6 and find similar results. Changing the mesh resolution while keeping the DEM resolution equal (Fig. 7g,h) results in a ratio image that is everywhere very close to 1.0. Changing the DEM resolution (Fig. 7c,f,i) leads to large positive ratio values of up to 1.4, particularly for the flatter regions in the northern part of the study area.

A last thing to consider is that the mesh resolution defines the frequency-resolving capability of an SEM model. The maximum and mean-resolved frequencies for each DEM-derived topographic surface model vary across different mesh resolutions (Fig. 8). The means of the resolved surface frequencies are also indicated with thinner lines in the same pattern. It can be seen that fine meshes are able to resolve higher frequencies compared to coarse meshes. It is important to realize that despite the fact that models with a 90-m and 270-m mesh seem to give very similar results, the frequency content is quite different.

Generally, seismic wavespeed increases with depth; therefore, it is often needed to coarsen the grid in the deeper parts of the model to retain a similar number of gridpoints per wavelength (Komatitsch and Tromp, 1999). We adopted a constant velocity model with representative upper crustal velocities. Because we have no significant sediments in the area (Shafique, van der Meijde, and Rossiter, 2011) and our model is relatively shallow, these velocities are valid for depths used in our model. Some variation might be possible because of composition differences, but the near-surface wave velocities are not expected to differ more than 20%–30% of the values used in this study. Our results can therefore be generalized for other velocity models. If velocities in other areas are much different in than the model we used, higher velocities will lead to longer wavelengths, and it is possible a slightly coarser mesh will still result in acceptable accuracy. For slower velocities, it might be necessary to use a smaller mesh to have the same accuracy presented in this article.

In summary, one can state that models with a mesh and DEM resolutions of 540 m and greater lead to unrealistic results when compared with the highest possible resolution models. Models with a resolution of 270 m and finer give comparable results, whereas changes in DEM resolution have more impact on the output models than changes in mesh resolution. It should be noted that these results might be dependent on the spatial scale of the topography and the ruggedness of the terrain. Results on mesh and DEM resolution are therefore valid for comparable terrains, but might not be directly applicable in regions with distinctly different geomorphological characteristics. It must be noted that the criteria of acceptability in this study are arbitrary and one may choose higher or lower acceptance values for all the spatial and statistical analysis.

Conclusion

Studies for simulation of topography-related seismic amplification rely strongly on the resolution of the topographic model as well as the modeling mesh. In this study, we analyzed how coarse a mesh and/or DEM resolution can be and still maintain accuracy compared to the most well-resolved case. We tested models of different mesh and

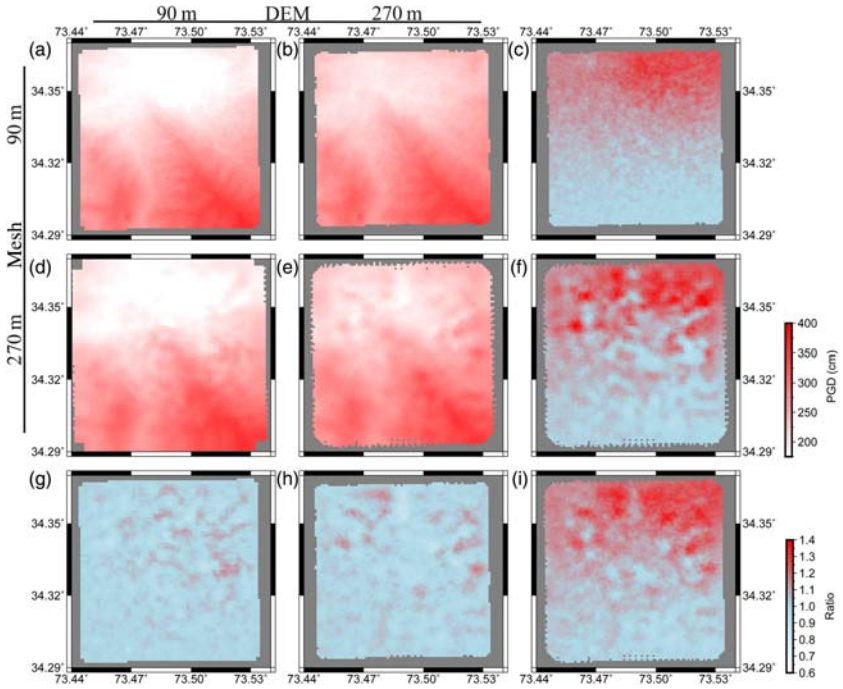

Figure 7. Ratios between models of 90 and 270 m mesh and DEM resolutions. (g) is product of (a) m90d90 and (d) m270d90, (h) plot of (b) m90d270 and (e) m270d270, (i) plot of (a) m90d90 and (e) m270d270, (f) plot of (d) m270d90 and (e) m270d270, and (c) plot of (a) m90d90 and (b) m90d270. The color version of this figure is available only in the electronic edition.

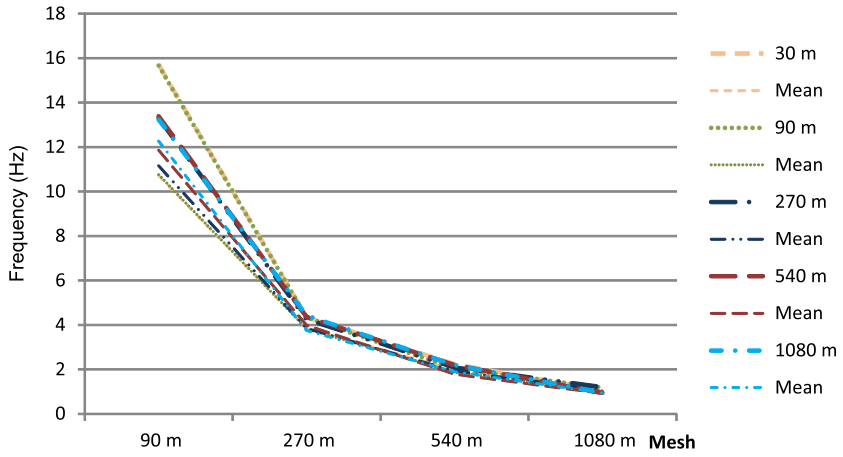

Figure 8. Maximum and mean frequencies resolved at topographic surface of the model for 90, 270, 540, and 1080 m resolution meshes. The color version of this figure is available only in the electronic edition.

DEM resolutions and compared it with the highest resolution possible (in our case, a model with a mesh of 90 m and a DEM of 30 m). Our results and analysis show that models with a resolution of 270 m and finer give comparable results, whereas changes in DEM resolution have more impact on the output models than changes in mesh resolution. Any model with a mesh and/or DEM resolution of 540 m or coarser produces inaccurate results compared with the highest resolution model with a 90 m mesh and a 30 m DEM.

It was found that in finer resolutions, abundance of topographic irregularities resulted in a destructive interference in some locations and hence resulted in lower amplitudes compared to those coming from coarse resolution. When the DEM/mesh resolution is relatively coarser, irregularities are smoothed and destructive interferences are reduced, resulting in higher amplitudes. Results on mesh and DEM resolution are valid for comparable terrains, but might not be directly applicable in regions with distinctly different geomorphological characteristics.

Data and Resources

More information about the light detection and ranging (lidar) can be obtained from https://lta.cr.usgs.gov/lidar_digitalelevation (last accessed June 2016). More information about the Global 30 Arc-Second Elevation (GTOPO30) model can be obtained from https://lta.cr.usgs.gov/GTOPO30 (last accessed January 2016). Advanced Spaceborne Thermal Emission and Reflection Radiometer (ASTER) global digital elevation model (GDEM) data were downloaded from Land Processes Distributed Active Archive Center (LP DAAC) Global Data Explorer http://gdex.cr.usgs.gov/gdex/ (last accessed June 2016). More information about Cubit can be found at Sandia National Laboratories website https://cubit.sandia.gov/ (last accessed August 2015). More information about SPECFEM3D Cartesian (devel version) was downloaded from the Computational Infrastructure for Geodynamics (CIG) website https://geodynamics.org/cig/software/specfem3d/ (last accessed August 2015). The centroid moment tensor (CMT) of the 2005 Kashmir earthquake was acquired from the Global CMT website http://www.globalcmt.org/ (last accessed October 2016). Generic Mapping Tools (GMT) was used for visualization of the results http://gmt.soest.hawaii.edu/ (last accessed May 2017).

Acknowledgments

The authors are grateful to Emanuele Cassaroti (Istituto Nazionale di Geofisica e Vulcanologia [INGV], Rome, Italy) for his help and support in mesh designing. The authors also thank Islam Fadel (International Institute for Geo-Information Science and Earth Observation [ITC], University of Twente, The Netherlands) for his help with the visualizations. Gratitude is extended to two reviewers, Arthur Rodgers and an anonymous reviewer,

whose critical comments and suggestions improved the quality of this article.

References

Assimaki, D., E. Kausel, and G. Gazetas (2005). Wave propagation and soil–structure interaction on a cliff crest during the 1999 Athens earthquake, *Soil Dynam. Earthq. Eng.* **25,** nos. 7/10, 513–527.

Bouchon, M., C. A. Schultz, and M. N. Toksöz (1996). Effect of three-dimensional topography on seismic motion, *J. Geophys. Res.* **101,** no. B3, 5835–5846.

Bouckovalas, G. D., and A. G. Papadimitriou (2005). Numerical evaluation of slope topography effects on seismic ground motion, *Soil Dynam. Earthq. Eng.* **25,** 547–558.

Dhanya, J., M. Gade, and S. T. G. Raghukanth (2017). Ground motion estimation during 25th April 2015 Nepal earthquake, *Acta Geod. Geophys.* **52,** no. 1, 69–93.

Hartzell, S. H., L. C. David, and W. K. Kenneth (1994). Initial investigation of site and topographic effects at Robinwood Ridge, California, *Bull. Seismol. Soc. Am.* **84,** 1336–1349.

Hough, S. E., J. R. Altidor, D. Anglade, D. Given, M. G. Janvier, J. Z. Maharrey, M. Meremonte, B. S. L. Mildor, C. Prepetit, and A. Yong (2010). Localized damage caused by topographic amplification during the 2010 M 7.0 Haiti earthquake, *Nature Geosci.* **3,** 778–782.

Jaiswal, K., D. Wald, P. Earle, K. Porter, and M. Hearne (2009). Earthquake casualty models within the USGS Prompt Assessment of Global Earthquakes for Response (PAGER) system, *Proc. of the Second International Workshop on Disaster Casualties*, University of Cambridge, United Kingdom, 15–16 June 2009.

Komatitsch, D., and J. Tromp (1999). Introduction to the spectral element method for three-dimensional seismic wave propagation, *Geophys. J. Int.* **139,** no. 3, 806–822.

Kramer, S. L. (1996). *Geotechnical Earthquake Engineering*, Pearson Education India, New Delhi, India.

Kumagai, H., T. Saito, G. O'Brien, and T. Yamashina (2011). Characterization of scattered seismic wavefields simulated in heterogeneous media with topography, *J. Geophys. Res.* **116,** no. B03308, doi: 10.1029/2010JB007718.

Lee, S. J., Y. C. Chan, D. Komatitsch, B. S. Huang, and J. Tromp (2009). Effects of realistic surface topography on seismic ground motion in the Yangmingshan region of Taiwan based upon the spectral-element method and LIDAR DTM, *Bull. Seismol. Soc. Am.* **99,** 681–693.

Lee, S. J., H. W. Chen, Q. Liu, D. Komatitsch, B. S. Huang, and J. Tromp (2008). Three-dimensional simulations of seismic wave propagation in the Taipei basin with realistic topography based upon the spectral-element method, *Bull. Seismol. Soc. Am.* **98,** 253–264.

Lee, S. J., D. Komatitsch, B. S. Huang, and J. Tromp (2009). Effects of topography on seismic-wave propagation: An example from northern Taiwan, *Bull. Seismol. Soc. Am.* **99,** 314–325.

Maufroy, E., E. Chaljub, F. Hollender, J. Kristek, P. Moczo, P. Klin, E. Priolo, A. Iwaki, T. Iwata, V. Etienne, *et al.* (2015). Earthquake ground motion in the Mygdonian basin, Greece: The E2VP verification and validation of 3D numerical simulation up to 4 Hz, *Bull. Seismol. Soc. Am.* **105,** doi: 10.1785/0120140228.

Shafique, M., M. van der Meijde, N. Kerle, and F. van der Meer (2011). Impact of DEM source and resolution on topographic seismic amplification, *Int. J. Appl. Earth Obs. Geoinf.* **13,** 420–427.

Shafique, M., M. van der Meijde, N. Kerle, F. van der Meer, and M. A. Khan (2008). Predicting topographic aggravation of seismic ground shaking by applying geospatial tools, *J. Himal. Earth Sci.* **41,** 33–43.

Shafique, M., M. van der Meijde, and D. G. Rossiter (2011). Geophysical and remote sensing-based approach to model regolith thickness in a data-sparse environment, *Catena* **87,** no. 1, 11–19.

Smith, M. J., J. Rose, and S. Booth (2006). Geomorphological mapping of glacial landforms from remotely sensed data: An evaluation of the principal data sources and an assessment of their quality, *Geomorphology* **76,** 148–165.

Sørensen, R., and J. Seibert (2007). Effects of DEM resolution on the calculation of topographical indices: TWI and its components, *J. Hydrol.* **347,** 79–89.

Spudich, P., M. Hellweg, and W. H. K. Lee (1996). Directional topographic site response at Tarzana observed in aftershocks of the 1994 Northridge, California, earthquake: Implications for mainshock motions, *Bull. Seismol. Soc. Am.* **86,** S193–S208.

Takemura, S., T. Furumura, and T. Maeda (2015). Scattering of high-frequency seismic waves caused by irregular surface topography and small-scale velocity inhomogeneity, *Geophys. J. Int.* **201,** 459–474.

Vaze, J., J. Teng, and G. Spencer (2010). Impact of DEM accuracy and resolution on topographic indices, *Environ. Model. Softw.* **25,** 1086–1098.

Wu, S., J. Li, and G. H. Huang (2008). A study on DEM-derived primary topographic attributes for hydrologic applications: Sensitivity to elevation data resolution, *Appl. Geogr.* **28,** 210–223.

Faculty of Geo-Information Science and Earth Observation (ITC)
University of Twente
P.O. Box 217
7500 AE Enschede, The Netherlands
s.khan@utwente.nl
m.vandermeijde@utwente.nl
(S.K., M.v., H.v.)

National Centre of Excellence in Geology (NCEG)
University of Peshawar
25120 Peshawar
Khyber Pakhtunkhwa, Pakistan
(M.S.)

Manuscript received 4 July 2016;
Published Online 25 September 2017